MAUSAM, **74**, 3 (July 2023), 607-620

MAUSAM

DOI :https://doi.org/10.54302/mausam.v74i3.1383
Homepage: https://mausamjournal.imd.gov.in/index.php/MAUSAM

UDC No. 551.581.1 : 551.588.16

Linking the solar cycle and Earth's climate

RAJASRI SEN JAISWAL, M. VINOTHA, K. THIRUMALA LAKSHMI and M. SIVA

Centre for Study on Rainfall and Radio Wave Propagation, Sona College of Technology, Salem, Tamil Nadu – 636 005, India

(*Received 17 August 2021, Accepted 12 December 2022*)

e mails : rajasrisenjaiswal@gmail.com; rajasrisenjaiswal@sonatech.ac.in

सार — **इस शोध पत्र में, लेखकों ने एल नीनो / ला नीना और विश्व में अकाल के समय एक स्थान पर वर्षा और तापमान के संदर्भ में पृथ्वी की जलवायु पर सौर चक्र के प्रभाव की जांच करने का प्रयास किया है। अध्ययन से पता चलता है कि पीक सनस्पॉट संख्या** (SSN) **अक्सर जोड़े में होती है। अक्सर कई चरम घटनाएँ भी देखी जाती हैं। ला निना कई चरम घटनाओं का अनुसरण करता है, या कभी-कभी इससे जुड़ा होता है। एल नीनो आमतौर पर सौर मिनीमा के बाद होता है, हालांकि यह हमेशा नहीं होता । इस अध्ययन से पता चलता है कि** SSN **ट्रफ** 2020 **में होगा।** 2023-2028 **के दौरान मल्टीपल** SSN **शिखर होने की संभावना है, इस अवधि के दौरान ला-नीना का पूर्वानुमान किया गया है। दुनिया के विभिन्न हिस्सों में अकालों पर ऐतिहासिक डेटा का एक प्लॉट कई** SSN **चरम और बहुत उच्च** SSN **मानों के बाद उनकी घटना को दर्शाता है। अध्ययन से पता चलता है कि कुल सौर विकिरण** (TSI) SSN **के साथ एक सुदृढ़ सहसंबंध रखता है। इसके अलावा,** SSN **और** TSI **के बढ़ने से ब्रह्मांडीय किरणों का प्रवाह कम हो जाता है।** SSN, TSI, **और तापमान के मासिक और वार्षिक बदलाव वर्षों में बढ़ती प्रवृत्तियों को दर्शाते हैं, जो वर्षों में बढ़ती उष्णाता का संके त देते हैं। हालांकि, इनमें से कोई भी प्राचल स्वतंत्र रूप से या एक साथ तापमान के साथ महत्वपूर्ण सहसंबंध नहीं रखता है,जिसका अर्थ है कि तापमान निर्धारित करने के लिए कुछ अन्य कारक भी जिम्मेदार हैं। अध्ययन से पता चला है कि वर्षा और** SSN **के बीच कोई सीधा संबंध नहीं है। हालाँकि, कई वर्षों में दोनों के बीच समान प्रवृत्ति दिखाई दी है। जांच से पता चला है कि विश्व की जलवायु पर सौर चक्र का प्रत्यक्ष प्रभाव पड़ता है।**

ABSTRACT. In this paper, the authors have made an effort to investigate the impact of the solar cycle on Earth's climate in the context of rainfall and temperature over a location, on El Nino/ La Nina, and world famines. The study shows that the peak sunspot number (SSN) often occurs in pairs. Multiple peaks are also seen frequently. The La Ninas follow multiple peaks, or sometimes associated with it. The El Ninos usually follow the solar minima, though not always. This study shows that the SSN trough will occur in 2020. The multiple SSN peak is likely to occur during 2023-2028, predicting a La-Nina during this period. A plot of historical data on famines in different parts of the world seems to show their occurrence after multiple SSN peaks and very high SSN values. The study shows that the total solar irradiance (TSI) bears a strong correlation with the SSN. Besides, the cosmic ray flux decreases as the SSN and the TSI increases. The monthly and yearly variations of SSN, TSI and temperature show increasing trends over the years, indicating increased warming as the years advance. However, none of these parameters bears significant correlations with the temperature, either independently or together, implying that some other factors are also responsible for determining the temperature. The study shows no direct relationship between rainfall and the SSN. However, several years show a similar trend between the two. The investigation indicates direct influence of the solar cycle on world climate.

Key words – El Nino, Famine, La Nina, Rainfall, Sunspot number, Temperature.

1. Introduction

Rainfall is perhaps the most important natural phenomenon ever known to impact the socio-economic arena of the world. It has the potential to flourish any civilization or wipe it off. Many civilizations have collapsed due to insufficient rainfall and the shift of rainfall regime. However, understanding the rainfall mechanism has been a challenge since time immemorial. Rainfall dynamics is a complicated aspect that depends on local meteorological elements, *viz*., temperature, pressure, relative humidity, wind speed, and direction at the surface and in the upper air. It also depends on several other parameters, say the proximity to the oceanic body, orography and latitude of a location, etc., to name a few. A study by Sen Jaiswal *et al*., (2013) shows that cloud liquid water, precipitation water, and latent heat are the key factors controlling the rainfall over a location.

Besides, atmospheric teleconnections, *viz*., the El Nino, and the La Nina that originate in the Central Pacific affect the climate at a far-off place (Alexander, 2002). The El Nino and the La Nina are the intricate weather patterns over the tropical Pacific Ocean, resulting from a periodic variation in sea surface temperature and wind speed (Neelin *et al*., 1998; Wallace *et al*., 1998; Wang and Picaut, 2004; Chang *et al*., 2006). It is a sea-saw kind of pattern. When the sea surface temperature is high over the eastern Pacific, it is less over the western Pacific and vice versa. Park *et al*., (2010) reported higher than average rainfall in the Indian subcontinent following an El Nino event. A study (Kane, 2006) in NE Brazil associates severe droughts with El Nino. Significant reductions in rainfall had happened in Australia following El Nino (Taschetto and England, 2009). Lin and Qian (2019) have shown the global impact of El Nino on temperature and precipitation anomalies.

By realizing the tremendous impact of the El Nino and La Nina on the climate at any place on Earth, the authors aim to search for its origin. By learning that the phenomenon occurs at a particular time of the year and shows periodicity, in this paper, the authors attempted to look for its origin in the solar cycle.

The Sun is the primary driving force of the atmospheric processes on Earth. It is well known that revolution of the Earth around the Sun, combined with the Obliquity of Ecliptic, gives rise to seasons. Several studies (Arnold and Robinson, 1998; Eddy, 1980; Engels and Geel, 2012) have revealed the influence of the solar cycle on Earth. Sir William Herschel indicated a possible impact of the solar cycle on the Earth's atmosphere (Herschel, 2012). The total solar irradiance (TSI) that is the incoming solar radiation at the top of the atmosphere, and the amount of solar radiation reaching the Earth's surface cause weather and climate on the Earth. The amount of radiation reaching a particular place on Earth depends on the Earth's orbital motion and its spin (Singh, 2006). Thus, changes in the Earth's atmospheric processes depend on solar radiation and the orbital and spinning motion of the Earth.

Besides, the cosmic rays of galactic and solar origin also affect the atmospheric processes (Ferrari and Szuszkiewicz, 2009).

The magnetic activity of the Sun controls the total solar irradiance (TSI). The sunspot number (SSN) is a manifestation of the level of the activity of the Sun. When the Sun is magnetically active, then the SSN is high (Maunder, 1894). Then, the TSI is higher (Eddy, 1980) than when it is magnetically quiescent (Xu *et al*., 2017). During the Sun's magnetically active period, more radiations emit from the Sun in the UV and visible regions (Arnold and Robinson, 1998). At this time, solar winds and solar flares are strong. The magnetic field around the Earth is also strong. Then, the cosmic rays, which are the high-energy protons and atomic nuclei (Imagine the Universe, 2020) coming from the Sun and outside the solar system, cannot penetrate the Earth's atmosphere as the strong magnetic field around the Earth reflects them into space. The measured intensity of cosmic rays shows high during the magnetically quiescent state of the Sun (Rosendahl *et al*., 2005). During the solar minima, when the solar wind is less, the Earth is more prone to cosmic rays that produce tiny aerosol particles after reaching the Earth. These aerosol particles act as cloud condensation nuclei (CCN) for cloud formation (Mukherjee, 2008). This phenomenon, in turn, affects Earth's albedo and precipitation. Mukherjee (2008) opines that during a high cosmic ray episode, the possibility of cloud formation and precipitation increases. The cosmic rays produce 14C (Engels and Geel, 2012). Thus, during the magnetically dormant period, there is more 14C (Engels and Geel, 2012). During a solar minimum, the decrease in the UV light received from the Sun leads to a reduction in the ozone concentration allowing more UV light to reach the Earth's surface.

A study shows that UV light breaks up the Ozone in the lower stratosphere (SPACE, 2013). The removal of Ozone causes cooling, which increases the temperature difference between the equatorial and the polar region in the lower stratosphere and the upper troposphere. The differential temperature between the equator and the pole is one of the major driving forces of the atmospheric heat engine. Thus, the removal of Ozone by the UV light appears to affect the atmospheric flow (SPACE, 2013).

Vieira *et al*., (2006) have found that the geomagnetic field and the ionizing potential of the cosmic rays control the effect of the Sun in influencing the Earth's environment. During the active state of the Sun, an electron beam traveling towards the Earth induces an ionizing current in the ionosphere. Mukherjee (2006) and Lehtinen *et al*., (1997) have reported that the ionizing current modulates the atmospheric temperature.

Hiremath (2006) has demonstrated a link between rainfall in India and sunspot activity. He (Hiremath, 2006) has shown that rainfall in India is higher when the Sun is magnetically weak. However, Bhattacharya and Narasimha (2005) found higher rainfall associated with a magnetically strong Sun. Bhalme *et al*., (1981) have investigated the correlations between the sunspot activity and surface meteorological elements over India. They (Bhalme *et al*., 1981) have reported a negative correlation between annual mean temperature, and sunspot and a

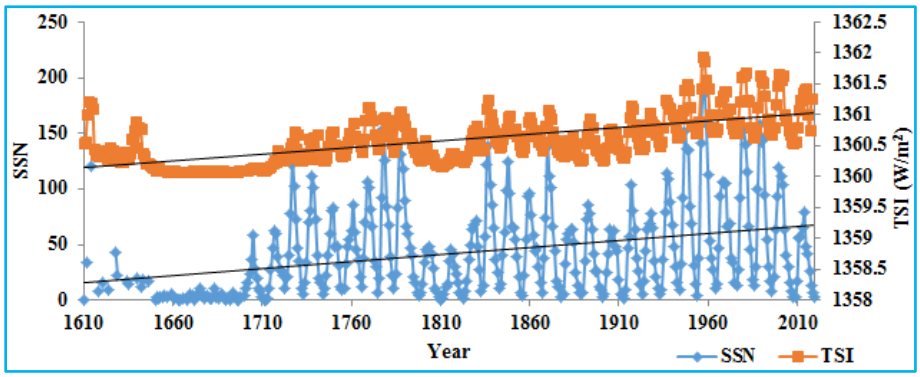

Fig. 1. The yearly variation of SSN (1610-2020) and TSI (1610-2018)

positive correlation between the daily sunspot and maximum temperature. They (Bhalme *et al*., 1981) found a negative correlation between sunspot number and annual surface pressure. Loon and Meehl (2008) noticed that during the solar maxima, the surface temperature in the Pacific Ocean shows a pattern conducive to La Nina. Studies show that the humidity (Oskomov *et al*., 2016) and temperature are strongly correlated to the sunspot number.

The Sun shows a periodicity in its cycle. Hathaway (2010) has demonstrated that SSN maxima occur after 11 years. When the Sun passes through the magnetically quiescent phase, marked by low sunspot number (Maunder, 1894), it radiates less energy, and the Earth also receives less heat. It is evident from the fact that the Earth had seen the Little Ice Age during the Maunder minimum (Maunder, 1894) in 1645-1715 when the snow prevailed throughout the year at low latitudes, the ice-free rivers froze. Therefore, there is enough evidence that the Sun controls the Earth's atmosphere.

In this paper, the authors have attempted to study the solar cycle in terms of the sunspot number (SSN), the total solar irradiance (TSI) and the cosmic ray flux. The study also investigates the effect of solar activity on the climatic conditions of India. The authors have studied the cosmic ray flux over Oulu, Finland, and Ahmedabad in the purview of the TSI and the SSN. An attempt has been made, in particular, to understand whether there is any link between the solar cycle and the El Nino/La Nina. The study also brings out the link between the occurrence of world famines with high SSN. The study predicts a La Nina in 2023-2028 and an El Nino in 2019-2020.

2. Materials and methods

The study in this paper includes sunspot number (SSN), total solar irradiance (TSI), all India temperature, and rainfall data. The study also includes an investigation of temperature and cosmic ray flux over Ahmedabad, India, and cosmic ray flux over Oulu, Finland. The authors have obtained the sunspot number (SSN) data (SIDC, 2020) during the period 1700-2020 from the Solar Influences Data analysis Center (SIDC), Royal Observatory of Belgium, the historical SSN data during the period 1610-1710 from the existing literature (Eddy, 1980) and the all India annual and monthly rainfall data and the annual temperature data (Open Government Data, 2016) during the period of 1901-2014 from the Open Government Data (OGD) Platform, India. They have obtained the all India monthly temperature data for the period 1901-2014 from the India Meteorological Department (IMD), the temperature data over Ahmedabad for the period 1901-2002 from the India Water Portal (India Water Portal, 2018) and El Nino and the La Nina years for the period 1900-2019 (www.stormfax.com/elnino.htm) from the National Oceanic and Atmospheric Administration (NOAA). The authors have obtained the list of famines from Waldford (1878), Kim and Guha-Sapir (2012), Eshaq *et al*. (2017), Hasell and Roser (2017) and Maxwell and Hailey (2021). The study also includes total solar irradiance (TSI) data over the period 1610-2018 obtained from the Interactive Solar Irradiance Data Centre, University of Colorado website (LASP, 2020). They have got the cosmic ray flux data over Oulu, Finland for the period 1964-2014 and over Ahmedabad for the period 1957-1973 (with some data gaps) from the Cosmic Ray Station, Sodankyla Geophysical Observatory, University of Oulu (Cosmic Ray Station, 2018) and the World Data Centre for Cosmic Ray, Physical Research Laboratory, Ahmedabad, India (ISEE, 2018), respectively.

The authors have fitted the yearly average values of these parameters to several models, *viz*., linear, cubic, power, quadratic, exponential, growth, lognormal, sigmoid, logarithmic, inverse and logistic to find out the

TABLE 1

The trend of SSN, all India temperature and rainfall

Slot of 20 years	SSN	Rainfall	Temperature
1901-1920	I	I	D
1921-1940	I	I	D
1941-1960	I	I	I
1961-1980	I	D	I
1981-2000	D	D	I
2001-2014	D	I	D (insignificant)
1900-2014	I	D (insignificant)	I

I-Increasing; D-Decreasing

correlations between them. They have judged the validity of the model by the F test at a 5% level of significance.

3. Results

3.1. *Variation of sunspot number*

Fig. 1 shows the variation of SSN with the year from 1610-2020. Fig. 1 indicates that the SSN undergoes cycles of changes with prominent peaks and troughs. The SSN gradually increases from a low value, reaches its peak, and again gradually decreases to a minimum. The same cycle repeats over and over again. The peaks represent the solar maxima, *i.e*., the most active period of the solar cycle. Fig. 1 also shows prominent troughs representing the solar minima, *i.e*., when the Sun passes through the most quiescent phase.

Fig. 1 reveals that the solar maxima show a definite periodicity, with an average period of 11.14 years. The period, however, varies between 8 (1761-1769) - 16 (1788-1804) years. Fig. 1 indicates that during 1650-1700, and 1710-1713, the SSN was very low. The SSN was 3, 0, 0 and 2, respectively, in 1710, 1711, 1712 and 1713. The year 1810 also had witnessed 0 SSN.

SSN minima occur after an average period of 11 years (Fig. 1). At times, the period is as long as 13 years (1843-1856), and as low as 9 years (1766-1775; 1775-1784).

Besides, Fig. 1 indicates that the SSN peak often occurs with a secondary peak of a little less magnitude. The period of such binary peaks is 11.14 years. Sometimes, multiple peaks of relatively comparative scale occur in three consecutive years. The investigation shows that the multiple peaks arise after 10-14 years. Some of the multiple peaks occurred in the following

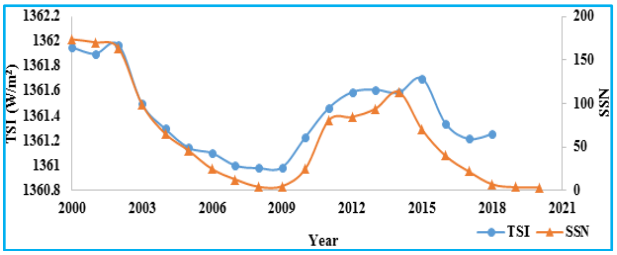

Fig. 2. The yearly variation of mean SSN (2001-2020) and TSI (2001-2018)

years: 1787-1789, 1803-1805, 1815-1817, 1828-1830, 1836-1838, 1847-1849, 1859-1861, 1870-1872, 1892-1894, 1905-1907, 1926-1928, 1937-1939, 1947-1949 and 1989-1991. During 1700-1745, multiple significant peaks were absent. It is noteworthy that the period 1645-1715, the so-called Maunder minimum (Maunder 1894), which is the Little Ice Age, was void of multiple SSN peaks.

Fig. 1 further shows that there is an increasing trend in sunspot numbers with year. A closer look at Fig. 1 shows increasing trends of SSN during 1700-1800, 1800-1900 and 1900-2000.

To know if the Sun's activity always showed a rising trend, the authors investigated the SSN over slots of 20 years from 1610-2020. The investigation shows that during these 20-year slots, sometimes the SSN showed a decreasing trend, while at times, an increasing trend was seen. Table 1 shows the trend of SSN during 1901-2014. It is noteworthy that the SSN showed a decreasing trend during 2001-2020 (Fig. 2). Trends from 1610-1900 are not shown.

The authors have investigated the monthly average SSN values in a particular year to understand the monthly variations in SSN. The investigation shows that the SSN reaches its maxima/minima in different months in different years (results not shown). The study further reveals that as the months advance from January to December, the SSN shows an increasing trend in some years. However, in some years, a decreasing trend is observed (results not shown).

To know how the SSN varies in a particular month over the years, they analyzed its variations during 1901-2020. Fig. 3 shows the result for December. Fig. 3 reveals an increasing trend. The investigation shows that each month, there is an insignificantly increasing trend in SSN over the years (results not shown). However, the SSN showed a decreasing trend in each month from 2010-2020, except May when an insignificantly decreasing trend is seen (results not shown).

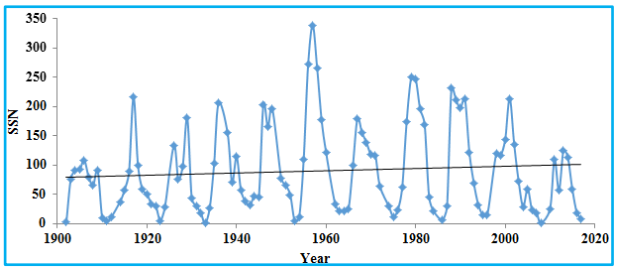

Fig. 3. The yearly variation of mean SSN in December (1901-2020)

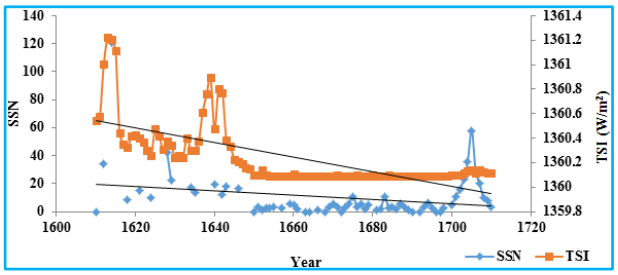

Fig. 4. The yearly variation of TSI and SSN (1610-1710)

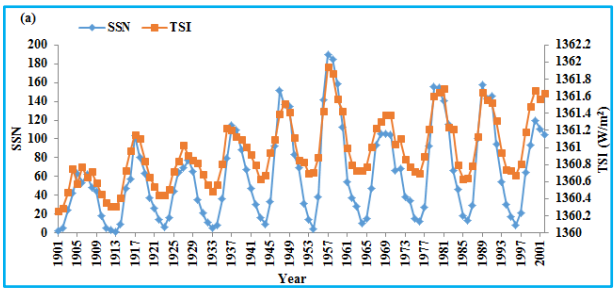

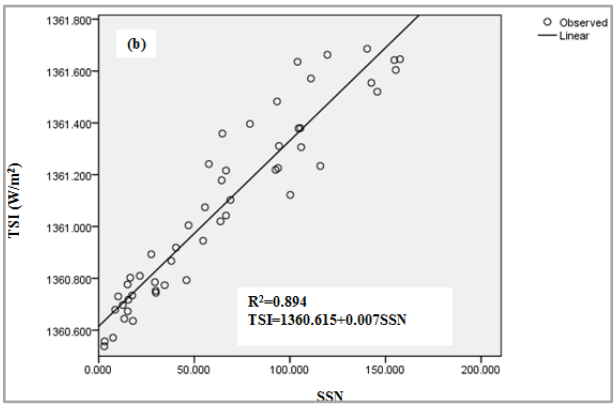

Figs. 5(a&b). The yearly variation of (a) TSI and SSN (1901-2002) and (b) correlation between SSN and TSI (1964-2014)

3.2. *TSI and SSN*

The authors have investigated the time series of the yearly average TSI from 1610-2018, and SSN from 1610-2020 (Fig. 1), to know if the two follow the same trend. Fig. 1 shows that like the SSN, the TSI showed an increasing trend during 1610-2018. A closer look at Fig. 1shows that like the SSN, the TSI showed an increasing trend in 1700-1800, 1800-1900 and 1900-2000, while from 2001-2018, both indicated a decreasing trend (Figs. 1-2). It is noteworthy that both showed a decreasing trend during 1610-1710 (Fig. 4). This finding appears to be due to the Maunder minimum (Maunder 1894) from 1645-1715.

Fig. 5(a) shows the trend of TSI and SSN from 1901-2002. Fig. 5(a) indicates that in almost all years, the crests (troughs) of the TSI time series exactly fall on that of SSN, implying an excellent correlation between the two. Besides, Fig. 5(a) reveals an increasing trend of SSN and TSI during 1901-2002.

The authors have analyzed the yearly average values of these parameters over slots of 20 years, to know if these parameters showed similar short-term trends. The study shows increasing trends of both parameters in all 20-year slots except during 1981-2000 (result not shown) and 2001-2020 (Fig. 2), when both the SSN and TSI showed decreasing trends. The investigation reveals that TSI and SSN are strongly correlated. Ambelu *et al.*, (2011) found a quadratic relation between SSN and TSI with an R^2 of 0.97.

The yearly average TSI and SSN values over the period 1700-2014 have been fitted to various models, like linear, cubic, quadratic, exponential, logistic, logarithmic, sigmoid, power, lognormal, inverse, and growth to know whether the TSI and SSN bear any significant correlations with each other. The authors have judged the validity of the relationship by the F test at a 5% level of significance. The investigation shows that the TSI and SSN bear a very significant linear relationship with an R^2 value of 0.894 over the period 1964-2014 [Fig. 5(b)], while over the period 1700-2014, the R^2 value is found to be 0.662 (result not shown). It appears that the less significant relationship between the two during 1700-2014 is due to the Maunder minimum (Maunder, 1894) from 1645-1715.

3.3. *SSN, TSI and cosmic ray*

Next, the authors attempted to determine the correlations between the SSN/TSI and cosmic ray flux. For this purpose, they chose two locations: Ahmedabad, India, and Oulu, Finland. The authors fitted the yearly averages of these quantities over Ahmedabad from 1957-1973 and Oulu from 1964-2014, to the curve estimation technique by considering the cosmic ray flux as the dependent, and the SSN as the independent variable. The study reveals that over Oulu [Fig. 6(a)], the cosmic ray flux and the SSN show a quadratic relation ($R^2 = 0.748$).

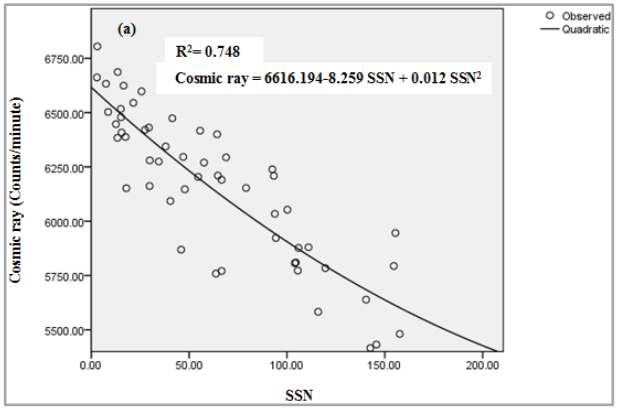

Figs. 6(a&b). Cosmic ray *versus* SSN over (a) Oulu, Finland and (b) Ahmedabad, India

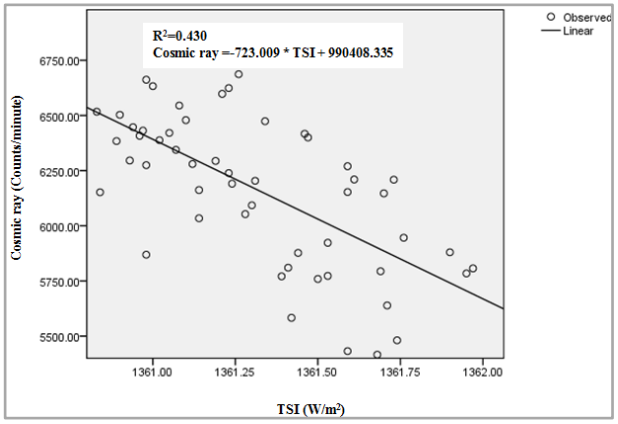

Fig. 7. TSI versus cosmic ray over Oulu, Finland

Over Ahmedabad [Fig. 6(b)], a cubic relation is found between the two with an R^2 of 0.952. The investigation shows that as the SSN increases, the cosmic ray flux decreases. Utomo (2017) has found the same result. He (Utomo, 2017) has reported that the solar wind, the amount of which depends on solar activity, reduces the cosmic ray flux that enters the Earth's surface. Harrison

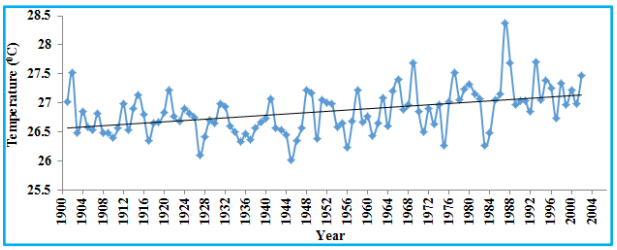

Fig. 8. The yearly variation of temperature over Ahmedabad (1901-2002)

(2008) has opined that the cosmic ray and solar activity are inversely related.

The cosmic ray flux bears a significant correlation with TSI over Ahmedabad when the cosmic ray is entered into the curve estimation technique as the independent parameter and the TSI as the dependent one. The corresponding R^2 value is 0.919 (result not shown). However, the two do not show any correlations when the TSI is considered as the independent parameter (result not shown). Over Oulu, the two bear a linear relation (R^2 = 0.43) when TSI is entered into the curve estimation as the independent parameter (Fig. 7). The curve estimation shows a linear relation over Oulu, with an R^2 of 0.43 by considering the cosmic ray flux as the independent variable.

Even though considering the cosmic ray flux as the independent variable yields higher R^2 values, it appears that the TSI governs the cosmic ray flux on the Earth's surface.

Linear regression by considering the yearly cosmic ray flux as a function of TSI and SSN shows a strong correlation with an R^2 of 0.747 over Oulu. However, over Ahmedabad, a poor correlation is seen. This may be because of the availability of fewer data. Frohlick *et al*., (2005) have reported that the magnetic field associated with solar activity affects the cosmic ray and the total solar irradiance.

It is noteworthy that the collision of the cosmic ray with the molecules of the atmosphere produces secondary ions that act as cloud condensation nuclei (CCN). The CCN further controls the radiation (Utomo, 2017) reaching the Earth's surface and forming rain.

3.3.1. *Dependence of temperature on SSN, TSI and cosmic ray flux at a location*

To know if the temperature over a location follows the trend of SSN/TSI, the authors analyzed the trend of these parameters over Ahmedabad from 1901-2002. Fig. 8

shows the pattern of temperature over Ahmedabad during 1901-2002. Figs. 5(a) and 8 reveal that during 1901-2002, all three parameters showed an increasing trend. Besides, Figs. 5(a) and 8 show that the peaks (troughs) of the temperature time series sometimes superpose on the peaks (troughs) of SSN/TSI. At times, however, the crests of one fall on the troughs of the other. The parameters show the same results in all the 20-year slots (result not shown).

To investigate the correlations between temperature and these parameters, if any, the yearly average temperature data during 1901-2002 over Ahmedabad; and the average annual TSI and SSN data for the corresponding years have been fitted to various models as described above. The investigation shows that the temperature does not bear any significant relationship with the TSI and SSN over Ahmedabad (results not shown).

To find out the parameter that can explain the temperature variability at a location, the authors have attempted to investigate the cosmic ray flux data over Ahmedabad. The cosmic ray flux data over Ahmedabad are available over the period 1957-1973 with some data gaps. The yearly average cosmic ray and the yearly average temperature data throughout the period of study have been fitted to various models, as described above. However, the temperature and the cosmic ray flux do not show any correlations (results not shown).

Next, the authors attempted to find out whether the temperature can be explained by any two/ three of these parameters-TSI, SSN, and cosmic ray flux. For this purpose, the authors fitted the yearly average cosmic ray flux, the SSN, the TSI, and the temperature data over the period 1957-1973 over Ahmedabad to linear regression. In the linear regression, a combination of two and all three parameters were considered independent and the temperature was the dependent variable. The investigation did not reveal any correlations in any cases, implying that TSI, SSN, and cosmic ray alone cannot explain temperature. The authors repeated the study over Ahmedabad from 1901-2002 to check if any correlation exists between temperature and TSI/SSN. However, they did not find any relationships.

The above results indicate that though the temperature often shows a similar trend as TSI and SSN, these alone cannot predict the temperature. It also depends on other factors, like surface albedo, latitude, altitude, distance from the sea, ocean current and prevailing wind. The dependence of temperature on surface albedo (UCAR, 2017) is given by:

$$T = \left[\frac{TSI(1-a)}{\sigma}\right]^{\frac{2}{4}} \quad (1)$$

where a is albedo; T is the temperature, and σ is Stefan-Boltzmann constant.

During the active cycle of the Sun, the SSN is high. High SSN is associated with high total solar irradiance at the top of the atmosphere, implying that the Earth's surface's insolation is also high. On the other hand, the insolation depends on the latitude of a location (Singh, 2006). The farther a place is from the equator (higher latitude), the more slant the solar ray strikes the Earth's surface, thereby intercepting a larger surface area on the ground. Thus, the insolation (energy incident/area/time) also reduces. Over the equator, the solar ray strikes at 90°, offering the shortest path to it to reach the location. Thus, insolation is the maximum at the equator. At the equator, the solar ray intercepts the shortest column of the atmosphere. Therefore, the energy lost due to atmospheric absorption, and scattering is also the least at the equator (Singh, 2006). At higher latitudes, the atmospheric column that the ray intercepts is thicker than at lower latitudes. Thus, the loss of energy due to atmospheric components is higher. Thus, the equatorial locations record higher temperatures than the higher latitudes.

The insolation (UCSB Geography, 2017) is given by:

$$E = E_0 \cos_{\varphi} \quad (2)$$

Where E is insolation, E_0 is the solar constant (TSI), and φ is the solar zenith angle. The solar zenith angle depends on the latitude θ of the Earth's station, the solar declination (δ) and the hour angle of the Sun (h) given by (UCSB Geography, 2017).

$$\cos_{\varphi} = \sin\theta\sin\delta + \cos\theta\cos\delta\cos h \quad (3)$$

Solar declination (δ) depends on the axial tilt of the Earth w.r.t. its orbital plane around the Sun and the day of the year (UCSB Geography, 2017). It also varies with the season (UCSB Geography, 2017). It shows a normal distribution with the season, peaking in June, and falling off on either side (UCSB Geography, 2017). Dependence of solar declination on the season, in turn, implies a dependency of the solar zenith angle on the latter. This finding suggests that the insolation and consequently the temperature and other meteorological elements, like rainfall, depend on the season.

The seasonal variation in SSN is manifested in the seasonal change of total solar irradiance and in turn, temperature. It is noteworthy that the average insolation and the average temperature follow the same typical pattern w.r.t latitude-peaking at the equator and falling off gradually at higher and higher latitudes in both the hemispheres (Applet-magic, 2018).

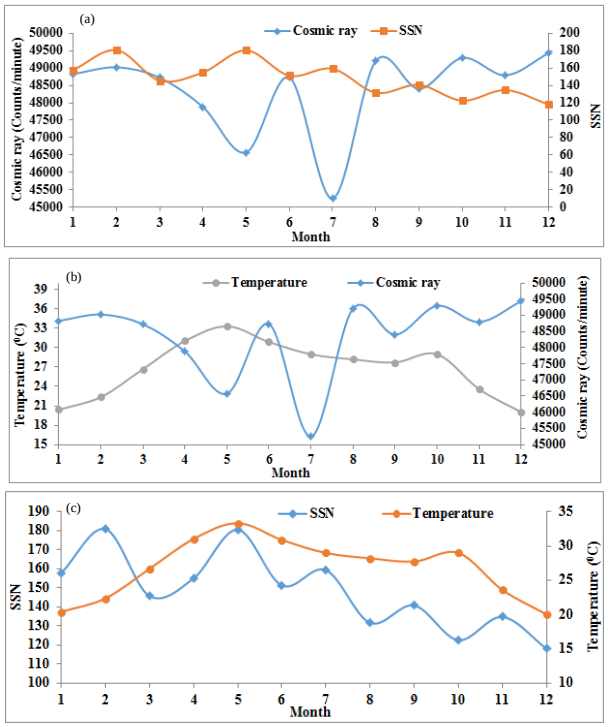

Figs. 9(a-c). Monthly variation of (a) SSN and cosmic ray over Ahmedabad, India (1970), (b) cosmic ray, and temperature over Ahmedabad, India (1970) and (c) of SSN and temperature over Ahmedabad, India (1970)

To investigate the seasonal variations of SSN, cosmic ray, and temperature, the authors have studied the monthly average values of these quantities over Ahmedabad in individual years from 1957-1973. Figs. 9 (a-c) respectively shows the seasonal variations of SSN, cosmic ray; cosmic ray, temperature; and SSN, the temperature in the year 1970. Figs. 9 (a-c) indicates that over Ahmedabad, the maximum (minimum) temperature occurs in May (January), while the maximum (minimum) SSN occurs in May (December). However, the maximum (minimum) cosmic ray flux occurs in December (July). Figs. 9 (a-c) also show the seasonal trends of these quantities in 1970. These reveal that the cosmic ray shows an increase, the SSN a decreasing, while the temperature shows an insignificantly increasing trend.

The investigation further reveals that the temperature and the SSN have always shown an opposite trend except1957 and 1958; so also the SSN and cosmic ray. The temperature and the cosmic ray have sometimes shown opposite trends, while at times, similar trends are seen (results not shown).

The crests and troughs of monthly average cosmic ray and SSN; and temperature and SSN over Ahmedabad mostly superpose, except 1957 and 1958. The crests and troughs of monthly average cosmic ray and temperature mostly superpose, except 1958, when in 50% of cases these two maintained the same phases.

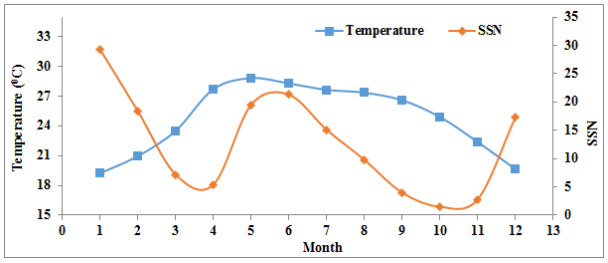

Fig. 10. Monthly variation of all India temperature and SSN (2007)

3.4. *Solar activity and all India temperature*

The authors analyzed the monthly temperature data over India and SSN from 1901-2020 to investigate the impact of solar activity on temperature. The investigation shows an increasing trend in December (Fig. 3). The variation of all India temperatures from January through December during the period shows that like the SSN, the temperature shows an increasing trend in all months (results not shown).

Variations of all India monthly temperature and the SSN in a particular year from 1988- 2007 show mostly the crests of one superpose with the troughs of the other. Very rarely, the crests (troughs) of one coincide with the crests (troughs) of the other (results not shown). It is interesting to notice the monthly variations in these two quantities in 2007 (Fig. 10). Fig. 10 shows that the crests of one are exactly superposed with the troughs of the other. The maximum SSN and the minimum temperature occurred in January. The maximum temperature had happened in May, while the SSN showed a high value in June. It is noteworthy that the year 2006-2007 was an El Nino year, while the year 2007-2008 was a La Nina year.

To examine whether it had always maintained an increasing trend, all India yearly temperature data have been investigated in slots of 20 years. The investigation reveals an increasing trend in some slots, while in some other slots, a decreasing trend is seen (Table 1). Table 1 reveals that the period 1901-1920 and 1921-1940 had seen a decreasing trend in temperature, the period 1941-1960, 1961-1980 and 1981-2000 had seen a sharp increasing trend, while the period 2001-2014 showed an insignificantly decreasing trend in temperature.

Besides, Table 1 shows that sometimes the SSN and temperature show a similar trend, while at times, an opposite trend is seen.

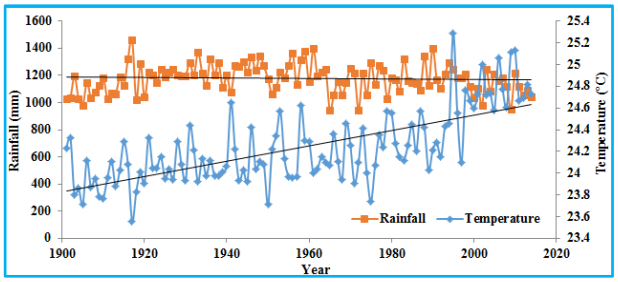

Fig. 11. The variation of all India rainfall and temperature (1901-2014)

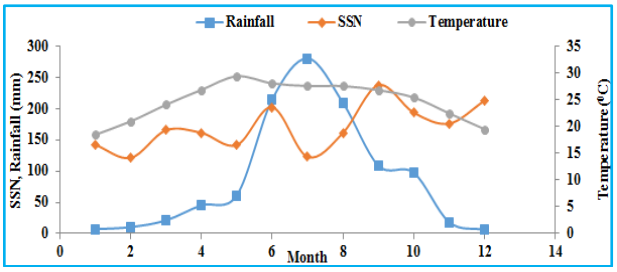

Fig. 12. Monthly variation of SSN, all India rainfall, and temperature (2001)

3.5. *Dependence of all India rainfall on Solar activity and all India temperature*

To find the influence of solar activity on rainfall, the authors have investigated the SSN, the all-India rainfall, and the all-India temperature from 1901-2014. Fig. 11 shows the yearly variations of rainfall and temperature over the period studied. It shows that there is an insignificant decreasing trend in rainfall and a significantly increasing trend in temperature during the period.

To find out whether the rainfall always maintained the same trend throughout, or it varied over different periods, the authors have analyzed the all India rainfall data in slots of 20 years, during 1901-2014. The investigation indicates that during the period 1901-1920, 1921-1940, 1941-1960 and 2001-2014, the rainfall showed an increase, while the period 1961-1980 and 1981-2000 showed a decreasing trend (Table 1).

Besides, Table 1 indicates that the SSN and rainfall show a similar pattern in some slots, while some 20-year slots show an opposite trend. The analysis of all India rainfall and SSN from 1988-2007 reveals that the peaks (troughs) of the rainfall time series sometimes match with the peaks (troughs) of SSN. However, at times, they do not match (results not shown).

Fig. 12 shows the time series of the SSN, temperature, and that of rainfall in the year 2001. Fig. 12 reveals that in 2001, the peak rainfall and the minimum SSN had occurred in July, while the maximum temperature had occurred in May. Besides, Fig. 12 reveals that the SSN, the all-India rainfall and temperature do not indicate a prominent similarity in the trend. The same result is seen in other years also (results not shown).

To find out a functional relationship between the SSN and rainfall; SSN and temperature, if any, the authors have fitted these parameters during 1901-2014 against several models, *viz.*, linear, cubic, power, growth, quadratic, exponential, lognormal, sigmoid, logarithmic, inverse and logistic. They have judged the validity of the model by the F test at a 5% level of significance. However, no two parameters show any correlations. It is noteworthy that India is a country of diverse climatology and geography. Thus, one needs to investigate the relationships between the SSN and other meteorological parameters over individual locations, instead of considering India as a whole.

3.6. *Solar activity and El Nino/La Nina*

By realizing the fact that the revolution of the Earth about the Sun causes season, and the insolation governs the atmospheric heat engine; causes ocean circulation; controls the global temperature, etc., it appears that the Sun is the sole controlling factor of the weather and the climate on the Earth. In this paper, the authors have attempted, in particular, to know whether the Sun causes the El Nino/ La Nina- one of the major factors influencing global rainfall and temperature. For this purpose, they have investigated the history of El Nino/La Nina years during the period 1900-2019 (STORMFAX, 2019). Analysis of SSN (SIDC, 2020) in Table A1 and El Nino/La Nina years (STORMFAX, 2019) in Table A2 shows that whenever the SSN multiple peaks had occurred, the La Nina followed (Table A2). Tables A (1 and 2) show that almost all the multiple peak occurrences were associated with La Nina in the following years and sometimes, in the same years. For example, the multiple SSN peaks occurred during 1905-1907, and La Nina had set in during 1906-1907.

Similarly, multiple SSN peaks happened in 1917-1919, and La Nina had occurred during 1916-1917 and 1920-1921. However, a few La Nina years were not associated with multiple peaks. The observation requires further investigation.

It is noteworthy that during the year 1700-1745, multiple prominent peaks were absent. However, historical data on El Nino/La Lina for the above period

were not available, to find out whether La Nina was missing during 1700-1745.

A close investigation on the El Nino/La Nina years (Table A2) and the SSN (Table A1) reveals that whenever the SSN trough had occurred, the El Nino followed in the following year. Sometimes, it happened in the same year, *viz*., SSN trough had occurred in the year 1902 and the year 1902-1903 witnessed an El Nino. SSN trough had occurred in the year 1913 and 1914-1915 was an El Nino year. The authors observed the same result in almost all years. However, it is noteworthy that some of the El Ninos were associated with peak solar activity.

From this study, it appears that solar activity causes El Nino and La Nina. Probably, the higher irradiance reaching the Earth during the peak SSN period and the lower irradiance during the SSN minima, when the Sun is in the quiescent phase, cause pressure imbalance in the central Pacific, in the East-West direction, giving rise to El Nino and La Nina. However, the exact mechanism is yet to find.

The energy emitted from the Sun causes convection current in the ocean, in the vertical direction (Aquatic, 2018). This current is further affected by the temperature gradient between the equator and the poles, causing ocean water flow across latitudes. The Coriolis force drifts the ocean current to the right in the northern and left in the southern hemisphere. The present paper shows that the energy received by the Earth's surface depends on the sunspot number, which, in turn, depends on the solar activity, implying that the ocean current, *viz*., the El Nino and the La Nina also depend on solar activity.

Studies (Loon and Meehl, 2008; Loon *et al*., 2007) show that during the peak sunspot activity, the sea surface temperature in the Pacific Ocean shows a pattern similar to that during a La Nina event. However, the study of Haam and Tung (2012) did not establish the link between the two.

Fig. 2 shows an expected decreasing trend of SSN during 2001-2020. Fig. 2 shows that the SSN will attain its minimum value in 2020 and an El Nino is likely to occur in the year 2019-2021. Likewise, the study predicts a multiple SSN peak episode in the year 2023-2028, predicting a La Nina during this period.

3.7. *Sunspot number and world famine*

An investigation of world famines during 1900-2017 [Waldford, 1878; Kim and Guha-Sapir, 2012; Eshaq *et al*., 2017; Hasell and Roser, 2017; Maxwell and Hailey, 2021] and the sunspot number (SIDC, 2020) shows that the years, which had witnessed very high SSN and the peak SSN, had seen significant famines also, *viz*., SSN peak occurred in 1727 and it had seen famine. The year 1769 had seen the peak SSN, followed by very high SSN values in the years 1770 and 1771. The devastating Great Bengal Famine, which had killed 10 million people in India and present Bangladesh, had occurred during 1769-1773 (Hunter 1868). The occurrence of famines (Waldford, 1878; Kim and Guha-Sapir, 2012; Eshaq *et al*., 2017; Hasell and Roser, 2017; Maxwell and Hailey, 2021) in other years associated with high/peak SSN is seen in Table A1. It appears that the occurrence of famines associated with peak SSN is due to the high irradiance during the Sun's active cycle, but full mechanism is not yet known.

4. Conclusions

The present paper investigates the solar cycle and aims to discover its impact on India's climate. The article further aims to ascertain the influence of the solar cycle on the El Nino and the La Nina.

The solar activity exhibits periodicity; the solar maxima occur after a period of an average of 11.14 years, and the minima after 11 years. The peaks often occur in pairs, or sometimes multiple peaks are observed.

Interestingly, the La Ninas follow multiple peaks, or occasionally occur associated with it. The El Ninos often follow the solar minima, though not always. An investigation of world famines during 1900-2017 and the SSN shows that the years, which had witnessed very high SSN and the peak SSN, had seen significant famines also. However, the physical processes through which, solar activity may influence Earth's climate is not fully understood.

According to the finding in this paper, the multiple SSN peak will occur from 2023-2028. Thus, La Nina is likely to occur during this period. The present study also indicates that in 2020, the Sun will be in the most quiescent state, which will lead to an SSN trough.

The multiple SSN peaks and very high SSN appear to cause famines.

The yearly SSN shows an increasing trend over the years, so also the temperature, indicating more and more warming in the years ahead. The same pattern in temperature and SSN is found in each slot of 20 years, starting from 1901-2014. The period 2001-2014 shows a decreasing trend both in the SSN and the all India temperature. Thus, there appears a strong possibility of the influence of the SSN over global temperature. It seems that high solar activity increases the temperature, implying that when the Sun passes through the highly active period,

abundant insolation reaches the Earth, increasing the surface temperature.

The SSN and the TSI are strongly correlated. The cosmic ray flux is also strongly correlated to the TSI and SSN. The investigation shows that the cosmic ray flux decreases as SSN/TSI increases.

Though the temperature shows the same trend as the SSN/TSI, it does not bear any significant correlation with the SSN/TSI or the cosmic ray flux. This finding indicates that temperature at a location is also governed by other parameters, along with these parameters.

As per the findings in this paper, all India rainfall and the SSN do not show any direct correlations. Some years show a similar trend in the rain and the SSN; some years do not.

Thus, though there may be increasing anthropogenic contributions to global warming during the industrial era, an inherent cause of global warming exists in the solar cycle itself, presently close to 1/3rd of warming due to GHGs according to scientific estimates.

Acknowledgment

The authors wish to express their gratitude to Sona College of Technology, Salem, India, for providing the infrastructural facilities to execute the work. The authors thank the Solar Influences Data Analysis Centre (SIDC), Royal Observatory of Belgium for the sunspot number data, and the National Oceanic and Atmospheric Administration for the information on El Nino and Na Nina years. The authors also thank the India Meteorological Department for providing the all India rainfall and surface temperature data; the Interactive Solar Irradiance Data Centre, the University of Colorado for the total solar irradiance data; the Cosmic Ray Station, Sodankyla Geophysical Observatory, the University of Oulu for the cosmic ray data over Oulu; the World Data Centre for Cosmic Ray, Physical Research Laboratory, Ahmedabad for the cosmic ray data over Ahmedabad; the India Water Portal for the temperature data over Ahmedabad; and the Wikipedia for providing the list of famines.

Disclaimer : The contents and views expressed in this study are the views of the authors and do not necessarily reflect the views of the organizations they belong to.

References

Alexander, M. and Scott, J., 2002, "The influence of ENSO on air-sea interaction in the Atlantic", *Geophys. Res. Lett.*, **29**, 1-4.

Ambelu, T., Falayi, E. O., Elemo, E. O. and Oladosu, O., 2011, "Estimation of total solar irradiance from sunspot number", *Lat. Am. J. Phys. Educ*., **5**, 741-745.

Applet-magic website, 2018, http://www.applet-magic.com/insolation.htm.

Aquatic website, 2018, http://www.aquatic.uoguelph.ca/oceans/AtlanticOceanWeb/NACurrents/Causes.htm.

Arnold, N. F. and Robinson, T. R., 1998, "Solar cycle changes to planetary wave propagation and their influence on the middle atmosphere circulation", *Ann. Geophys*., **16**, 69-76.

Bhalme, H. N., Reddy, R. S., Mooley, D. A. and Ramana Murty, B. H. V., 1981, "Solar activity and Indian climate", *Proc. Indian Acad. Sci*., **90**, 245-262.

Bhattacharyya, S. and Narasimha, R., 2005, "Possible association between Indian monsoon rainfall and solar activity", *Geophys. Res Lett*., **32**, 1-5.

Chang, P., Yamagata, T., Schopf, P., Behera, S. K., Carton, D. J., Kessler, W. S., Meyers, G., Qu, T., Schott, F., Shetye, S. and Xie, S. P., 2006, "Climate fluctuations of tropical coupled systems-The role of ocean dynamics", *J. Clim*., **19**, 5122-5174.

Cosmic Ray Station website, 2018, http://cosmicrays.oulu.fi.

Eddy, J. A., 1980, "Climate and the role of the Sun", *J. Interdiscip. Hist*., **10**, 725-747.

Engels, S. and Geel, B. V., 2012, "The effects of changing solar activity on climate: Contributions from palaeoclimatological studies", *J. Sp. Weather Sp. Clim*., **2**, 1-9.

Eshaq, A. M., Fothan, A. M., Jensen, E. C., Khan, T. A. and Alamodi, A. A., 2017, "Malnutrition in Yemen: an invisible crisis", *The LANCET correspondence*, **389**, 31-32.

Ferrari, F. and Szuszkiewicz, E., 2009, "Cosmic rays: A review for astrobiologists", *Astrobiol. J*., **9**, 413-436.

Frohlick, C., Beer, J. and Muscheler, R., 2005, "Corelation between cosmic ray intensity and total solar irradiance during the last three solar cycles", *Americ. Geophys. Union*., SH41A-1110.

Haam, E. and Tung, K. K., 2012, "Statistics of solar cycle–la nina connection: correlation of two autocorrelated time series", *J. Atmos. Sci*., **69**, 2934-2939.

Harrison, R. G., 2008, "Discrimination between cosmic ray and solar irradiance effects on clouds and evidence for geophysical modulation of cloud thickness", *Proc. Royal Soc. Math. Phys. Eng. Sci*., **464**, 2575-2590.

Hasell, J. and Roser, M., 2017, "Famines" published online at OurWorldinData.org. Retrieved from: 'https://ourworldindata.org/famines' [Online Resources].

Hathaway, D. H., 2010, "The solar cycle",*Living Rev. Sol. Phys*., **7**, 1-65.

Herschel, S. W., 2012, "Scientific papers of Sir William Herschel at 100", *Astron. Geophys*., **53**, 2-13.

Hiremath, K. M., 2006, "The influence of solar activity on the rainfall over India: Cycle-to-cycle variations", *Astrophys. Astr*., **27**, 367-372.

Hunter, W., 1868, "The Annals of rural Bengal", University of Exeter**,** New York.

Imagine the Universe website, 2020, https://imagine.gsfc.nasa.gov/science/toolbox/cosmic_rays1.html.

India Water Portal website, 2018, https://www.indiawaterportal.org/met_data.

ISEE website, 2018, ftp://ftp.isee.nagoya-u.ac.jp/pub/WDCCR/STATIONS/AHMEDA.

Kane, R. P., 2006, "El Nino effects on rainfall in South America: Comparison with rainfall in India and other parts of the world", *Adv. Geosci*., **6**, 35-41.

Kim, J. J. and Guha-Sapir, D., 2012, 'Famines in Africa: is early warning early enough?", *Glob. Health Action*., **5**, 1-3.

LASP website, 2020, https://lasp.colorado.edu/lisird/data/tsi.

Lehtinen, N. G., Bell, T. F., Pasko, V. P. and Inan, U. S., 1997, "A two-dimensional model of runaway electron beams driven by quasi-electrostatic thundercloud fields", *Geophys. Res. Letter*., **21**, 2639-2642.

Lin, J. and Qian, T., 2019, "A new picture of the global impacts of the El Nino-Southern Oscillation", *Sci. Rep*., **9**, 1-7.

Loon, V. H. and Meehl, G. A., 2008, "The response in the Pacific to the Sun's decadal peaks and contrasts to cold events in the Southern Oscillation", *J. Atmos. Sol. Terr. Phys*., **70**, 1046-1055.

Loon, V. H., Meehl, G. A. and Shea, D. J., 2007, "Coupled air-sea response to solar forcing in the Pacific region during northern winter", *J. Geophys. Res*., **112**, 1-8.

Maxwell, D. and Hailey, P., 2021, "Analysing famine: The politics of information and analysis in food security crises", *J. Humanit. Affairs*, **3**, 16-27.

Maunder, W. E., 1894, "A prolonged sunspot minimum", *Knowledge: An Illustrated Magazine of Sci*., **17**, 173-176.

Mukherjee, S., 2008, "Cosmic influence on the Sun-Earth environment", *Sensors*, **8**, 7736-7752.

Mukherjee, S., 2006, "Influence of star flare on the Sun-Earth environment and its possible relationship with snowfall", *The EGGS News Lett*., **14**, 14-17.

Neelin, J. D., Battisti, D. S., Hirst, A. C., Jin, F. F., Wakata, Y., Yamagata, T. and Zebiak, S. E., 1998, "ENSO theory", *J. Geophys. Res*., **103**, 14261-14290.

Open Government Data website, 2016, WWW.Data.gov.in.

Oskomov, V. V., Sedov, A. N., Saduyev, N. O., Kalikulov, O. A., Naurzbayeva, A. Zh., Alimgazinova, N. Sh. and Kenzhina, I. E., 2016, "Cosmic rays intensity and atmospheric humidity at near earth surface", 5th International Conference on Mathematical Modeling in Physical Sciences, *Athens*, Greece, 2016.

Park, H. S., Chiang, J. C. H., Lintner, B. R. and Zhang, G. J., 2010, "The Delayed effect of major El Nino events on Indian monsoon rainfall", *J. Clim*., **23**, 932-946.

Rosendahl, I. M., Baumstark, K. C. and Rink, H., 2005, "Mutation induction in mammalian cells by accelerated heavy ions", *Adv. Sp. Res*., **36**, 1701-1709.

Sen Jaiswal, R., Neela, V. S., Fredrick, S. R., Rasheed, M., Zaveri, L. and Sowmya, V., 2013, "Identification of key parameters producing rainfall", *MAUSAM*, **64**, 281-296.

SIDC website, 2020, http://www.sidc.be/silso/datafiles.

Singh, S., 2006, "Climatology", Prayag Pustak Bhawan, Allahabad, 503

SPACE website, 2013, https://www.space.com/19280-solar-activity-earth-climate.html.

STORMFAX website, 2019, http://www.stormfax.com/elnino.htm.

Taschetto, A. S. and England, M. H., 2009, "El Nino Modoki impacts on Australian rainfall", *J. Clim*., **22**, 3167-3174.

UCAR website, 2017, https://scied.ucar.edu/planetary-energy-balance-temperature-calculate.

UCSB Geography website, 2017, https://www.geog.ucsb.edu/ideas/Insolation.html.

Utomo, Y. S., 2017, "Correlation analysis of solar constant, solar activity, and cosmic ray", *2nd International Symposium on Frontier of Applied Physics*, Jakarta, Indonesia, 2017.

Vieira, L. E. A. and Da, Silva, L. A., 2006, "Geomagnetic modulation of clouds effects in the southern hemisphere magnetic anomaly through lower atmosphere cosmic ray effects", *Geophys. Res. Lett.*, **33**, 1-5

Waldford, C., 1878, "The famines of the world: past and present", *J. Stat. Soc. London*, **41**, 433-535.

Wallace, J. M., Rasmusson, E. M., Mitchell, T. P., Kousky, V. E., Sarachik, E. S. and Storch, H. V., 1998, "On the structure and evolution of ENSO-related climate variability in the tropical Pacific: Lessons from TOGA", *J. Geophys. Res*., **103**, 241-259.

Wang, C. and Picaut, J., 2004, "Earth's Climate: The Ocean-Atmosphere Interaction", AGU, Washington D. C, 21-48.

Xu, J. C., Xie, J. L. and Qu, Z. N., 2017, "Relations between the sunspot numbers and total solar irradiance", *Astrophys. J*., **851**, 141-149.

Appendix

TABLE A1

Sunspot numbers during 1700-2020

Year	SSN	Year	SSN	Year	SSN	Year	SSN	Year	SSN	Year	SSN
1700	8.3	1754	20.3	1808	13.5	1862	112.1	1916	95	1970	148
1701	18.3	1755	16	1809	4.2	1863	83.5	1917	173.6	1971	94.4
1702	26.7	1756	17	1810	0	1864	89.2	1918	134.6	1972	97.6
1703	38.3	1757	54	1811	2.3	1865	57.8	1919	105.7	1973	54.1
1704	60	1758	79.3	1812	8.3	1866	30.7	1920	62.7	1974	49.2
1705	96.7	1759	90	1813	20.3	1867	13.9	1921	43.5	1975	22.5
1706	48.3	1760	104.8	1814	23.2	1868	62.8	1922	23.7	1976	18.4
1707	33.3	1761	143.2	1815	59	1869	123.6	1923	9.7	1977	39.3
1708	16.7	1762	102	1816	76.3	1870	232	1924	27.9	1978	131
1709	13.3	1763	75.2	1817	68.3	1871	185.3	1925	74	1979	220.1
1710	5	1764	60.7	1818	52.9	1872	169.2	1926	106.5	1980	218.9
1711	0	1765	34.8	1819	38.5	1873	110.1	1927	114.7	1981	198.9
1712	0	1766	19	1820	24.2	1874	74.5	1928	129.7	1982	162.4
1713	3.3	1767	63	1821	9.2	1875	28.3	1929	108.2	1983	91
1714	18.3	1768	116.3	1822	6.3	1876	18.9	1930	59.4	1984	60.5
1715	45	1769	176.8	1823	2.2	1877	20.7	1931	35.1	1985	20.6
1716	78.3	1770	168	1824	11.4	1878	5.7	1932	18.6	1986	14.8
1717	105	1771	136	1825	28.2	1879	10	1933	9.2	1987	33.9
1718	100	1772	110.8	1826	59.9	1880	53.7	1934	14.6	1988	123
1719	65	1773	58	1827	83	1881	90.5	1935	60.2	1989	211.1
1720	46.7	1774	51	1828	108.5	1882	99	1936	132.8	1990	191.8
1721	43.3	1775	11.7	1829	115.2	1883	106.1	1937	190.6	1991	203.3
1722	36.7	1776	33	1830	117.4	1884	105.8	1938	182.6	1992	133
1723	18.3	1777	154.2	1831	80.8	1885	86.3	1939	148	1993	76.1
1724	35	1778	257.3	1832	44.3	1886	42.4	1940	113	1994	44.9
1725	66.7	1779	209.8	1833	13.4	1887	21.8	1941	79.2	1995	25.1
1726	130	1780	141.3	1834	19.5	1888	11.2	1942	50.8	1996	11.6
1727	203.3	1781	113.5	1835	85.8	1889	10.4	1943	27.1	1997	28.9
1728	171.7	1782	64.2	1836	192.7	1890	11.8	1944	16.1	1998	88.3
1729	121.7	1783	38	1837	227.3	1891	59.5	1945	55.3	1999	136.3
1730	78.3	1784	17	1838	168.7	1892	121.7	1946	154.3	2000	173.9
1731	58.3	1785	40.2	1839	143	1893	142	1947	214.7	2001	170.4
1732	18.3	1786	138.2	1840	105.5	1894	130	1948	193	2002	163.6
1733	8.3	1787	220	1841	63.3	1895	106.6	1949	190.7	2003	99.3
1734	26.7	1788	218.2	1842	40.3	1896	69.4	1950	118.9	2004	65.3
1735	56.7	1789	196.8	1843	18.1	1897	43.8	1951	98.3	2005	45.8
1736	116.7	1790	149.8	1844	25.1	1898	44.4	1952	45	2006	24.7
1737	135	1791	111	1845	65.8	1899	20.2	1953	20.1	2007	12.6
1738	185	1792	100	1846	102.7	1900	15.7	1954	6.6	2008	4.2
1739	168.3	1793	78.2	1847	166.3	1901	4.6	1955	54.2	2009	4.8
1740	121.7	1794	68.3	1848	208.3	1902	8.5	1956	200.7	2010	24.9
1741	66.7	1795	35.5	1849	182.5	1903	40.8	1957	269.3	2011	80.8
1742	33.3	1796	26.7	1850	126.3	1904	70.1	1958	261.7	2012	84.5
1743	26.7	1797	10.7	1851	122	1905	105.5	1959	225.1	2013	94
1744	8.3	1798	6.8	1852	102.7	1906	90.1	1960	159	2014	113.3
1745	18.3	1799	11.3	1853	74.1	1907	102.8	1961	76.4	2015	69.8
1746	36.7	1800	24.2	1854	39	1908	80.9	1962	53.4	2016	39.8
1747	66.7	1801	56.7	1855	12.7	1909	73.2	1963	39.9	2017	21.7
1748	100	1802	75	1856	8.2	1910	30.9	1964	15	2018	7
1749	134.8	1803	71.8	1857	43.4	1911	9.5	1965	22	2019	3.6
1750	139	1804	79.2	1858	104.4	1912	6	1966	66.8	2020	8.8
1751	79.5	1805	70.3	1859	178.3	1913	2.4	1967	132.9		
1752	79.7	1806	46.8	1860	182.2	1914	16.1	1968	150		
1753	51.2	1807	16.8	1861	146.6	1915	79	1969	149.4		

TABLE A2

El Nino and La Nina years

El Nino Years	La Nina Years	El Nino Years	La Nina Years
1900-1901		1969-1970	1970-1971
1902-1903	1903-1904	1972-1973	1973-1974
1905-1906	1906-1907		1975-1976
	1908-1909	1976-1977	
1911-1912		1977-1978	
1914-1915	1916-1917	1982-1983	
1918-1919	1920-1921	1986-1987	1988-1989
1923-1924	1924-1925	1991-1992	
1925-1926	1928-1929	1992-1993	
1930-1931	1931-1932	1994-1995	1995-1996
1932-1933	1938-1939	1997-1998	1998-1999
1939-1940			2000-2001
1940-1941		2002-2003	
1941-1942	1942-1943	2004-2005	
1946-1947	1949-1950		early 2006
1951-1952		2006-2007	
1953-1954	1954-1955		2007-2008
1957-1958		2009	
1963-1964	1964-1965		late 2010 - early 2011
1965-1966		mid - late 2015	

Conflict of Interest : There is no conflicts of interest.